energy&fuels

pubs.acs.org/EF

Article

Dynamics of Asphaltene Aggregates under High-Pressure CO_2 Revealed by Pulsed-Field Gradient NMR

Evgeny V. Morozov,* Sergey N. Trukhan, Ivan V. Kozhevnikov, Ivan V. Peterson, and Oleg N. Martyanov

Cite This: *Energy Fuels* 2023, 37, 17215−17226

Read Online

ACCESS | Metrics & More | Article Recommendations

ABSTRACT: The work demonstrates the results of the first experimental PFG NMR study in situ of the complex phase behavior of asphaltenes in the presence of high-pressure CO_2. To perform the experiments, a series of sealed, thick-walled quartz capillaries were prepared with a mixture of CO_2 and asphaltenes dissolved either in chloroform or benzene at different initial concentrations. Then, the temperature dependence of the diffusion coefficients of the asphaltene aggregates was measured for each sample after the mixture reached its equilibrium state, at which, in accordance with the solubility limit, only part of the initial asphaltenes remained dissolved. Despite quite low residual asphaltene concentrations in solution, experimental data clearly demonstrated the presence of aggregated structures (up to 70−80 wt %) attributed solely to nanoaggregates, with no signs of the presence of macroaggregates in the samples. Temperature dependencies of aggregate diffusivity clearly showed that the scenario, according to which the evolution of the asphaltene aggregates will develop, strongly depends on the initial asphaltene concentration, mass fraction of CO_2 loaded into the system, and chemical nature of the solvent used. In particular, the most diluted asphaltene solution, expected to be the most resistive to the aggregation processes in a high-pressure CO_2 environment, revealed the most pronounced aggregation-dependent translational dynamics as compared to those with a moderate initial asphaltene concentration. Contrarily, the concentrated asphaltene solution may not show drastic aggregation processes if the mass fraction of the CO_2 loaded will not appear to be so high. Finally, the experimental results provide evidence that the temperature-triggered structural transformation of asphaltene aggregates due to the noncovalent bond breakup is not hindered under high-pressure CO_2, but instead becomes more emphasized. The results obtained shed new light on asphaltene aggregate dynamics and brought new knowledge about the fundamental behavior of asphaltene in high-pressure CO_2 conditions.

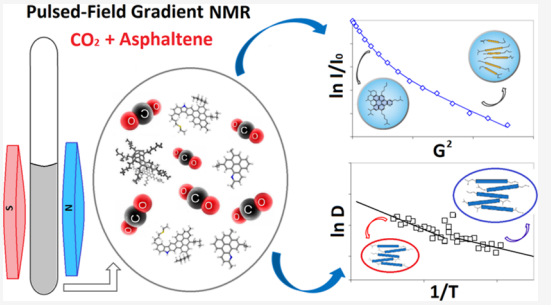

1. INTRODUCTION

The gradual depletion of conventional oil resources, along with the decline in the number of new oilfield discoveries, actively stimulates the petroleum industry and engineering toward increasing the efficiency of hydrocarbon recovery from a reservoir. It is well known that the residual oil saturation in reservoirs after the primary and secondary recovery stages may reach as much as 50−60% of the original-oil-in-place (OOIP).[1−4] Evidently, to meet the growing energy demand, oil recovery efficiency must be sufficiently increased. The most prominent approach which can greatly improve the efficiency of hydrocarbon recovery after primary and secondary oil production stages is the application of enhanced oil recovery (EOR) techniques.[1,5−7] This approach utilizes various processes such as thermal treatment, gas injection, and chemical flooding that modulate the fluid properties such as oil viscosity, miscibility, and interfacial tension of injected and reservoir fluids or affect the rock-fluid wettability.

Among the listed EOR methods, gas-based techniques seem to be the most attractive due to their low costs, high efficiency, and positive environmental impact. Thus, according to the US Department of Energy, gas injection accounts for nearly 60% of EOR production in the United States.[8] The gas EOR is based on the injection of carbon dioxide (CO_2), nitrogen (N_2), natural (mostly CH_4), and flue gases into an oil reservoir. Despite the diversity of gases which could be potentially used for EOR, mainly CO_2 injection has been actively used for decades in either academic studies or industrial practices due to its substantial effects on enhancing oil production.[9−12] These effects include oil viscosity reduction, oil swelling,

Received: July 31, 2023
Revised: October 18, 2023
Accepted: October 20, 2023
Published: November 2, 2023

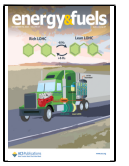

reduction of interfacial tension, partial extraction of light hydrocarbons, and increasing the mobility of crude oil, all of which results in improving the sweep and oil displacement efficiency.[9,10,13,14] It is important to note that the application of CO_2-EOR is also favorable due to substantial contribution to decreasing greenhouse gas emissions.[15,16]

Many advantages that CO_2-EOR provides during oil production are challenged by serious drawbacks associated with the undesirable deposition of heavy organic components in the crudes. Thus, injection of CO_2 into the formation alters the equilibrium conditions of the reservoir and fluid properties, which may result in the destabilization of asphaltenes.[17−19] Destabilized asphaltenes precipitate out of the crude oil, which causes pore throat plugging, decreasing the permeability, changing the wettability of the rock surface, further resulting in damaging the wellbore region, and a dramatic reduction in the recovery factor.[19−23] In addition to the downhole problems, precipitated asphaltenes form deposits on the internal surfaces of pipelines, pumps, oil tanks, and other surface facilities, which requires regular remediation procedures. Evidently, all this significantly increases the operating costs of oil production and processing, making them economically inefficient.[19] To meet the demand for higher oil recovery efficiency, a proper prediction of reservoir performance during the CO_2-EOR becomes of great importance, which cannot be achieved without a deep understanding of the processes contributing to asphaltene destabilization.

A key step in addressing the challenge of undesirable deposit formation is elucidating the complex physicochemical properties and phase behavior of asphaltenes in the presence of high-pressure CO_2. Asphaltenes are typically defined as the heaviest and most polar fraction of crude oil, which are insoluble in *n*-alkanes but can completely be dissolved in light aromatics like benzene and toluene.[24,25] This definition is widely accepted, though it poorly characterizes the phase behavior of dissolved asphaltenes. From a structural point of view, asphaltenes are considered to be formed by a system of polycondensed aromatic rings with aliphatic chains attached to them.[26,27] They can also contain some heteroatoms (such as nitrogen, sulfur, and oxygen) and metals in trace amounts (nickel and vanadium) in proportions depending upon the origin of the sample.[28] The complex molecular structure of asphaltenes determines their strong propensity toward self-association even in "good" solvents: the asphaltene molecules begin to form nanoscale (3−5 nm) aggregated structures at very diluted concentrations of 50−150 mg/L[29,30] or even lower,[31] which then undergo clustering at higher concentrations (2−5 g/L) with the formation of fractal particles in the size range of 5−10 nm.[32−34] Asphaltene aggregates appear quite stable, and no precipitation, either in crude oil or model solutions, usually occurs until the temperature, pressure, or chemical composition of the system is changed.[24,35−37] For example, the addition of *n*-heptane (or, more importantly, sub- or supercritical CO_2) to the asphaltene solution causes destabilization of aggregated structures and further increases their size up to a few microns, followed by asphaltene precipitation and deposit formation.[38−40] Since the formation of aggregates from the individual asphaltene molecules triggers the overall precipitation process in the presence of CO_2, primary attention should be focused on studying the aggregate dynamics and its phase behavior.

Many hundreds of research works dealt with asphaltenes, but the effects of CO_2 injection on the phase behavior of asphaltene aggregates are still poorly understood. From a practical point of view, the majority of experiments were carried out to observe deposition processes and reveal the onset of asphaltene precipitation, i.e., provide information about how much CO_2 can be injected into reservoirs before asphaltene begins to precipitate.[41−45] Similarly to this point, the kinetics of deposition were also studied, providing information about how much the rate of asphaltene precipitation depends on the mole fraction of injected CO_2, asphaltene concentration, temperature, and pressure.[23,38,39,46,47] However, information about the onset and rate of asphaltene precipitation is not sufficient for a deep understanding of the mechanisms of CO_2-induced asphaltene aggregation. Only a few studies were devoted to the latter issue. According to the results obtained, three general mechanisms of asphaltene aggregation in the presence of CO_2 were unveiled.

The first one is a mere decrease of asphaltene solubility upon dilution by carbon dioxide, which is similar to those widely observed when considering the flocculant (i.e., low molecular weight alkanes)-induced asphaltene precipitation.[48,49] Another relevant mechanism is associated with the role of resin acting as a peptizing agent for asphaltenes in crude oils:[50−52] injected supercritical (sc) CO_2 causes selective extraction of resin and/or reduction of the resin/asphaltene ratio, which leads to asphaltene destabilization followed by aggregation and eventual precipitation.[53] The last and much more specific mechanism that was not commonly presented in conventional asphaltene precipitation studies is the intermolecular interactions of carbon dioxide with asphaltenes. Thus, Gabrienko and co-workers found that asphaltenes containing C−O−R and S═O functional groups capable of specific Lewis acid−base interactions with CO_2 were observed to precipitate after CO_2 dissolution in crude oil.[54] Also, a larger number of oxygen-containing fragments and lower aromaticity in CO_2-induced asphaltenes were also observed.[55] Moreover, it was recently shown that the amine group can ultimately form an amide functional group through reaction with CO_2, disturbing asphaltene stability in the oil matrix.[56] The diversity of physical interactions and chemical reactions, which are both capable of triggering the cascade of asphaltene aggregate transformations into solid deposits in the presence of CO_2, does complicate the whole picture, which is still far from a complete understanding.

Unfortunately, despite the evident importance of this issue, asphaltene aggregates and their phase behavior are beyond the list of studies so far. To the best of our knowledge, none of the published articles considered directly the structure, local dynamics, phase behavior, or interactions of asphaltene aggregates in high-pressure CO_2 conditions by any of the experimental techniques. A very promising approach that could shed light on this issue is the application of modern experimental techniques in situ since only under such conditions will the new data obtained provide relevant information.[57] One of the experimental techniques which could probe the behavior of asphaltene aggregates in situ is pulsed-field gradient (PFG) NMR. This method appears to be superior for accurate measurements of translational motion (i.e., diffusion coefficients) and probing the structural and dynamic properties of the diffusing species, their interactions with the surroundings, and the spatial morphology of the network through which the diffusion path lies.[58] Since the PFG NMR method is inherently sensitive to the architecture of asphaltene aggregates, it has been successfully used previously

https://doi.org/10.1021/acs.energyfuels.3c02862
Energy Fuels 2023, 37, 17215−17226

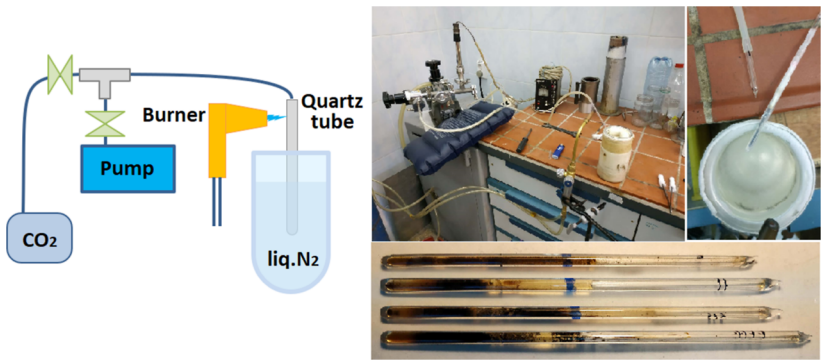

Figure 1. Procedure of sample preparation: a general scheme, photos of the assembled gas line, a quartz tube with frozen asphaltene solution + dry ice, and finally sealed capillaries.

Table 1. Samples of the Asphaltene + Solvent + CO_2 Mixture Sealed in Thick-Walled Quartz Capillaries

notation[a]	solvent	asphaltenes (mg)	solvent (mg)	CO_2 (mg)	initial asphaltene concentration (g/L)	mass fraction of CO_2 loaded (%)
Ch7	$CHCl_3$	0.8	181	122	7	40.2
Ch25	$CHCl_3$	2.9	175	105	25	37.1
Cd54	$CDCl_3$	4.2	117	94	54	43.7
Ch150	$CHCl_3$	17.9	185	70	150	25.7
B48	C_6H_6	3.9	72	87	48	53.4

[a]Ch, Cd, and B refer to normal chloroform, deuterated chloroform, and benzene, respectively.

for investigation of the aggregate size and aggregation mechanisms,[59−61] the interrelation between the structure and aggregation properties of asphaltenes,[62] and temperature-triggered structural rearrangement of asphaltene aggregates.[63] On the other hand, PFG NMR proved to be a highly efficient technique for diffusion measurements performed at high-pressure conditions, including $scCO_2$.[64,65] It makes the PFG NMR method the proper choice for studying the behavior of asphaltene aggregates in a high-pressure CO_2 environment.

To fill the gap in knowledge about asphaltene aggregate behavior under high-pressure CO_2 conditions, the first experimental PFG NMR study of model asphaltene solutions mixed with high-pressure carbon dioxide was carried out in situ. To perform the experimental measurements, a series of sealed, thick-walled quartz capillaries was prepared with a mixture of CO_2 and asphaltenes dissolved in deuterated chloroform, normal chloroform, and benzene at different initial concentrations. Then, the temperature dependence of the diffusion coefficients of asphaltene aggregates for every sample was measured after the mixture reached its equilibrium state, where only part of the initial asphaltenes remained dissolved according to the solubility limit. The results obtained demonstrate remarkable phenomena which have not been previously observed. Most importantly, it is clearly shown that the scenario according to which the evolution of the asphaltene aggregates will develop strongly depends on the initial concentration of dissolved asphaltenes and the mass fraction of CO_2 loaded into the system. We believe that the results of this work bring new knowledge about the fundamental behavior of asphaltene aggregates under high-pressure CO_2 that will contribute to an overall understanding of the phenomenon and assist in better prediction of reservoir performance during CO_2-EOR.

2. EXPERIMENTAL SECTION

2.1. Samples Preparation. Asphaltenes used in this work were extracted from heavy oil produced in Tatarstan Republic (Russia) following ASTM method D6560-00 (Standard Test Method for Determination of Asphaltenes (Heptane Insolubles) in Crude Petroleum and Petroleum Products).[66] The composition, properties, and phase behavior of asphaltenes extracted were comprehensively studied by numerous experimental techniques and were published earlier.[37,54,57,63,67−70] At the first stage of sample preparation, the solid asphaltenes were dissolved in deuterated chloroform (99.8% of D atoms in $CDCl_3$, Solvex-D), normal chloroform ($CHCl_3$, Merck), and benzene (C_6H_6, Merck) at different concentrations: 7, 25, 48, 54, and 150 g/L. All solvents used were of reagent grade or higher. It is necessary to note that the deuterated toluene-d_8, which is most commonly used for NMR measurements of asphaltene solutions, demonstrates some trace amount of the normal ($C_6H_5CH_3$) toluene, with the $-CH_3$ peak overlapping the proton signal of asphaltene aliphatic side chains. Since the signal under study appeared quite low due to the relatively small residual concentration of asphaltenes in the finally prepared samples, only those solvents were chosen which had a proton signal far away from the resonance signal of asphaltenes.

The development of appropriate in situ magnetic resonance methods for studying processes in the subcritical and supercritical states is associated with great technical difficulties. In particular, the sample must be placed in a radiofrequency circuit in an explosion-proof cell, which is made of a material that does not absorb RF/microwave radiation and has miniature geometric dimensions (an inner diameter of several millimeters). Perhaps only thick-walled glass/quartz, sapphire, and ceramic capillaries or tubes made of durable PEEK polymer satisfy the listed conditions, which can be used only at relatively low temperatures. The technical difficulties have now led to the absence of commercial systems which would allow one to use NMR methods at elevated temperatures and pressures (>30 atm), and a homemade approach was then developed to perform the measurements.

For long-term experiments on measuring the diffusion coefficients using PFG NMR, the long-term stability of the systems under study is of fundamental importance. In multicomponent systems, stability is easier to provide using completely insulated (sealed on both sides) thick-walled capillaries. This option allows performing the experiments in the mode of constant average density and different pressures, which depends on temperature. So, the second stage of the sample preparation consisted of the following steps, Figure 1: loading of the asphaltene solution into the capillary, freezing of the loaded solution

https://doi.org/10.1021/acs.energyfuels.3c02862
Energy Fuels 2023, 37, 17215−17226

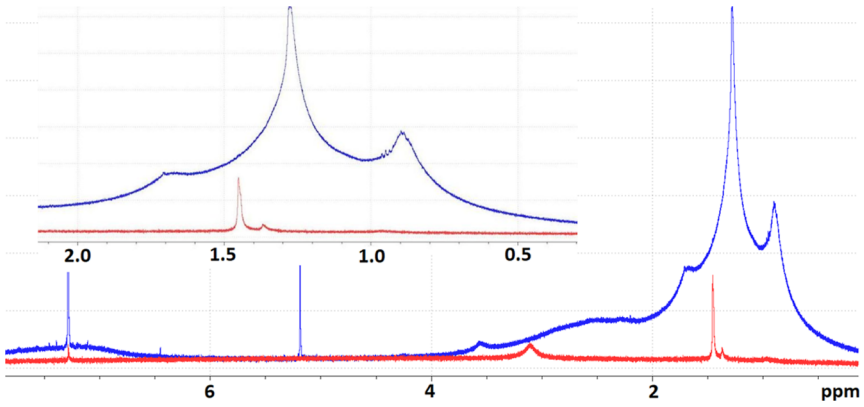

Figure 2. Proton spectra of 25 g/L asphaltene solution in $CDCl_3$ without carbon dioxide (blue line) and Cd54 solution in high-pressure CO_2 conditions (red line) recorded at 25 °C.

in liquid nitrogen, inlet of gaseous CO_2 into the system after preliminary vacuuming of the frozen asphaltene solution, condensing of CO_2 over a frozen solution in the form of dry ice (at the end of the capillary placed in liquid nitrogen), pumping out the gas line, and sealing of the top capillary end.

After dozens of sample preparation tests with quartz tubes with different inner (D_{in}) and outer (D_{out}) diameters, filled with a liquid with a known equation of state, it was established that the maximum pressure, $P_{explosion}$, which can withstand the capillary is determined by the ratio of D_{out}/D_{in} and also significantly depends on D_{in}. To work with the systems containing CO_2 near the critical point (31 °C, 73 atm), it is necessary that the capillaries withstand a pressure of at least 100 atm and at the same time have as large an internal diameter as possible in order to provide the highest possible signal-to-noise ratio when performing the NMR measurements. These conditions satisfactorily correspond to quartz tubes with dimensions of $D_{out}/D_{in} = 2$ at $D_{out} < 5$ mm.

As a result, a series of samples was prepared according to the procedure described. The initial asphaltene concentrations, type of solvent, and mass fraction of CO_2 loaded are listed in Table 1 for every sample. When the sealed capillaries reach room temperature, pressure inside the sample increases, which causes partial precipitation of the dissolved asphaltenes. Thus, only part of the asphaltenes remained dissolved according to the solubility limit; however, it was decided to retain the initial concentration value in the sample notation for convenience (Table 1). In addition to the studied mixtures, a reference CO_2 + $CDCl_3$ sample was prepared, which contained no asphaltenes. Prior to running the PFG NMR measurements inside the probe, all samples were tested at 60 °C to make sure they were explosion-proof.

2.2. PFG NMR Measurements and Data Analysis. PFG NMR experiments were carried out using a wide-bore Bruker AVANCE DPX 200 spectrometer with a magnetic field strength of 4.7 T, which corresponds to a 200.13 MHz proton resonance frequency, equipped with a GREAT 3/60 gradient unit, a z-gradient probe Diff50 capable of producing high-strength gradient pulses (up to 1800 G/cm) with short duration and ramp times, and a 10 mm proton RF coil. Due to strong gradient pulses, it became possible to keep the gradient pulse duration very short, avoiding sufficient signal loss from the least mobile molecules with the shortest spin−spin relaxation time T_2. The acquisition of ^1H spectra of the samples was carried out using a standard bore Bruker Avance III 600 spectrometer with a magnetic field strength of 14.1 T, corresponding to a 600 MHz proton resonance frequency, equipped with conventional spectroscopic probes.

The pulse sequence used for the diffusion measurements was a stimulated spin echo,[58] where the gradient pulse duration (δ) and the experimental observation time (diffusion time, Δ) were kept constant at 0.5 and 50 ms, respectively. The value of the pulsed field gradient (g) was varied from 0 to 250 G/cm to obtain sufficient signal attenuation. 16 linear gradient steps were used to obtain the signal decay, and >400 scans for each value of g were set up to provide a reasonable signal-to-noise ratio. As a result, the diffusion measurement data were recorded as a pseudo-2D spectrum containing the set of 1D spectra acquired at different values of the pulsed field gradient.

Long-time PFG NMR measurements (18−26 h span for one temperature point) of diffusing species in low-viscosity sub- or supercritical fluids require homogeneous temperature distributions to prevent bulk convection within the sample.[64] Therefore, special attention was paid to temperature control. Unfortunately, the air flow mode widely used in NMR probes for sample heating/cooling is highly prone to creating an inhomogeneous and unstable temperature distribution within the 5 mm NMR tube. To address this issue, a previously developed approach was used:[71] the temperature inside the probe was reached and then maintained by using the water circuit of the BCU 20 cooling unit, which provided superior temperature stability within the thick-walled quartz capillary (D_{in} = 2 mm) and minimized the possible temperature gradients. Yet the comparatively narrow channel inside the sealed capillary hindered any potential convection processes.

The gradient strength was calibrated by using a known diffusion coefficient of water in a H_2O/D_2O mixture. Prior to running the PFG NMR measurements, the sample was kept for 30 min or longer inside the probe at the designated temperature. Evidently, summing up an extremely long time of measurements, this ensured complete thermal equilibration. Taking into account the established values of $P_{exposion}$ for the thick-walled tubes used, the PFG NMR measurements were carried out in a temperature range of 8−42 °C. For this temperature range, the estimated values of pressure inside the sealed capillaries are as follows: 10 °C—45 atm, 20 °C—56 atm, 30 °C—71 atm, and 40 °C—82 atm.

To probe the mean displacement of the disusing species in a PFG NMR experiment, two gradient pulses with length (δ) and magnitude (g) are applied with a time separation (Δ) when the probed molecules are diffusing freely in space. In the case of translational self-diffusion and a single diffusion coefficient, the measured NMR signal attenuates according to a well-known Stejskal−Tanner expression[72]

$$I = I_0 \exp[-\gamma^2 g^2 \delta^2 D(\Delta - \delta/3)] \quad (1)$$

where I is the intensity of the signal, I_0 is the signal intensity at $g = 0$ (i.e., the signal intensity obtained at zero gradient strength), D is the self-diffusion coefficient, and γ is the gyromagnetic ratio of the resonating nucleus. In the case of single diffusing species, the logarithm of the normalized signal attenuation (I/I_0) versus $b = \gamma^2 g^2 \delta^2 (\Delta - \delta/3)$ results in a straight line with a slope D. Since the diffusing species in asphaltene solution should be presented by at least two different sorts of asphaltene structures (aggregated and nonaggregated ones), the signal attenuation decay is expected to be inherently biexponential or even more complex. Previously, it has been comprehensively discussed[63] that the results of numerous experimental studies on asphaltene solutions distinctly indicate the

https://doi.org/10.1021/acs.energyfuels.3c02862
Energy Fuels 2023, 37, 17215−17226

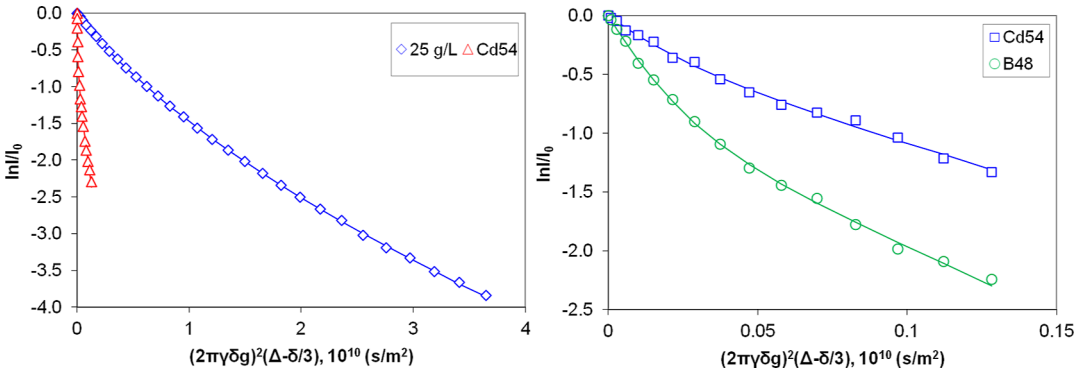

Figure 3. NMR signal attenuation decays of 25 g/L asphaltene solution in $CDCl_3$ without carbon dioxide and Cd54 solution in high-pressure CO_2 conditions recorded at 25 °C (a); comparison of the decays for Cd54 and B48 samples (b). Symbols are the experimental points; lines are two-component exponential fitting.

presence of bimodal aggregate size distribution with characteristic maxima in the range 1−3 and 5−7 nm. For this reason, a multiexponential analysis of the signal attenuation decays, $I/I_0 = f(b)$, based on a nonlinear least-squares fitting procedure, has been widely used in previous works, providing reliable results.[59,61,63,73]

3. RESULTS AND DISCUSSION

3.1. ^{1}H NMR Spectroscopy. It is well known that the majority of the protons in asphaltene molecules are located in aliphatic side chains on the periphery of the polycyclic aromatic hydrocarbons (PAHs) core, giving the characteristic group of broad overlapping lines at 0−3 ppm in the proton NMR spectrum.[55,74] Unlike the aliphatic part, the signal from the protons associated directly with the PAHs core is rather weak since their number is relatively small, yet the spin−spin relaxation times of aromatic protons are quite short due to proximity to the paramagnetic centers formed by either unpaired electrons of polycondensed aromatic rings or porphyrin complexes of vanadyl (VO^{2+}).[68,70] It makes a weak signal very broad, further decreasing its apparent intensity, so the principal analysis of the asphaltene behavior is to be performed using solely the aliphatic part of the spectra. As can be seen in Figure 2, the signal of the aliphatic part in the range of 0−3 ppm is indeed very strong, while the aromatic part in the range of 6.5−8 ppm is shown by the weak broad line, overlapping with the single line of residual $CHCl_3$.

Proton NMR spectra of the asphaltene solutions subjected to high-pressure carbon dioxide demonstrate significant differences in terms of the integral intensity and position of the spectral lines as compared to those in the samples without CO_2, Figure 2. First, twice less the diameter of the sealed quartz capillary causes a 4-fold decrease of the matter quantity within the RF coil (2 mm for the sealed sample vs 4.2 mm for the normal glass NMR tubes); second, approximately 50% dilution of the asphaltene solution by liquid CO_2 additionally results in a 2-fold decrease of the signal. Thus, due to these two factors only, the signal is expected to fade by an order of magnitude relative to the normal asphaltene solution. Carbon dioxide introduced into the mixture leads to asphaltene precipitation and deposition on the capillary walls. Since the NMR signal of the solid deposits is too broad to be visible in the narrow-band (10 ppm width) spectra, the narrow lines observed in Figure 2 (seen in the 1.3−1.5 ppm range) belong to asphaltenes remaining in solution and a small amount of water inevitably caught from the air moisture during sample preparation. The signal of water (1.45 ppm) overlaps the asphaltene aliphatic peaks and becomes clearly visible only in the reference sample containing no asphaltenes or in the B48 sample where benzene was used instead of chloroform. Its position (1.45 ppm) was found to be slightly shifted as compared to that in pure $CDCl_3$ (1.56 ppm) due to the presence of liquid CO_2. The spectral range, 1.3−1.5 ppm, was then used for recording the signal attenuation decays during the diffusion measurement presented below. Using the single line of $CHCl_3$ in $CDCl_3$ as a reference, the residual concentration of the asphaltenes was assessed to be about 2−4 g/L.

The decrease of asphaltene concentration in the sealed samples is accompanied by the almost complete disappearance of the signal from the H_α protons (seen as a broad shoulder at 2−3 ppm in normal asphaltene solution), corresponding to $-CH_3$ attached to aryl rings and aliphatic chain $-CH_2$ alpha to aromatics. Also, line narrowing and their slight drift can be found: the central asphaltene aliphatic peak shifts to the left side from 1.28 to 1.44 ppm, Figure 2. The disappearance of the broad shoulder in the spectrum appears similar to that previously observed during strong dilution of concentrated asphaltene solutions at ambient conditions.[63] Line drift and narrowing can be caused by the precipitation of PAHs, which are abundant with unpaired electrons and metalloporphyrins,[68,70,75] which lead to reduction of the paramagnetic contribution into the chemical shift of the lines and spin−spin relaxation time T_2. Indeed, there are three distinct types of paramagnetic species in asphaltenes that largely contribute to relaxation time shortening: ions of metals with partially filled d- and f-electronic shells (the most widely presented are vanadium and nickel), delocalized π-electrons of aromatic rings, and stable organic radicals of the side chains. The concentration of paramagnetic ions (e.g., VO^{2+} in metalloporphyrins) varies in a wide range (tens and hundreds of ppm), depending on the oil source, and can reach up to 0.1%,[76−78] while the concentration of stable carbon radicals might be 3−9 times lower.[79] However, despite this low content, the effect of paramagnetic species is enormous since the magnetic moment of the electron is ∼650 times larger than that of nuclei. As a result, the presence of a small amount of paramagnetic species strongly affects the relaxation time values; for example, it is enough to reduce T_2 of asphaltene aliphatic protons to tens of milliseconds,[80] whereas for common hydrocarbons, typical T_2 can be tens of seconds.

Analysis of the proton NMR spectra of all samples prepared revealed that neither initial asphaltene concentration nor

https://doi.org/10.1021/acs.energyfuels.3c02862
Energy Fuels 2023, 37, 17215−17226

temperature affect the character of the lines or their position. The only slight line broadening was observed in the Ch150 sample due to a decrease of sample homogeneity caused by the high amount of precipitated solid matter. It is necessary to note that employment of ^{13}C NMR spectroscopy to study sealed samples seems impossible without special isotope enrichment: the low natural abundance of ^{13}C (~1.1%) along with manifold signal attenuation due to capillary configuration and asphaltene precipitation both result in extremely weak signals and an impractical time of spectra acquisition.

3.2. PFG NMR Measurements. Measurements of the translational dynamics of asphaltenes revealed a remarkable difference in the diffusion curves of signal attenuation decays obtained for the sealed samples and normal asphaltene solution. Due to the low viscosity of the media where asphaltenes diffuse, the mobility of the species increases greatly, as can be seen when compared with the normal asphaltene solution: a decay obtained from the Cd54 sample declines very fast, while those from the normal solutions extend much farther, Figure 3a. The most important observation here is that the diffusion curve of the sealed sample is not a straight line in $\ln I/I_0$ vs b coordinates, i.e., the data obtained point to the presence of more than one diffusion component. It was previously shown that the diffusion curves of the normal asphaltene solution consist of two or three distinct components, depending on sample concentration, where the more mobile first component corresponds to less aggregated structures (referred to as "asphaltene monomers" for simplicity despite the possible presence of more complex structures), while the second and third (in concentrated solutions) ones correspond to nano- and macroaggregates, respectively.[63] The multiexponential analysis of the signal attenuation decays of the sealed samples provides the best fit in the following form:

$$I/I_0 = p_m \exp(-bD_m) + p_a \exp(-bD_a) \quad (2)$$

where p_m, D_m, and p_a, D_a are the weight fractions and diffusion coefficients of monomers and aggregates, respectively. Here, the term "monomers" refers to less aggregated asphaltene species and low-molecular impurities (such as trace amounts of water caught from the air during sample preparation), while "aggregates" actually refer to the complex aggregated structures formed by asphaltene molecules.

The appearance of more than one component in signal attenuation decays evidences that the aggregation processes occurred in asphaltene solution subjected to a high-pressure CO_2 environment, despite a quite low residual asphaltene concentration (few grams per liter). In other words, the small quantity of asphaltenes remaining in solution after destabilization and precipitation of a major part of the matter continues to form aggregated structures in the presence of high-pressure CO_2. This experimental fact is supported well by the results of molecular dynamics simulation, which indicate a strong tendency of asphaltenes to form nanoaggregates in high-pressure CO_2 conditions.[53] It is interesting to note that the solvent plays an important role in aggregation processes under high-pressure CO_2 conditions. Comparison of the signal attenuation decays of the Cd54 and B48 samples, where deuterated chloroform and benzene were used, respectively, shows that the weight fraction of aggregated structures, p_a, is in the range of 70−80% in the case of Cd54, while the benzene solution B48 revealed the presence of only 40−50% of aggregates. It can be explained by the greater affinity of the aromatic solvent to PAHs of asphaltene molecules, allowing a larger fraction of asphaltene molecules to remain in a low-aggregated state even in the presence of carbon dioxide. This finding is well consistent with the very recent observations on the ability of dilute concentrations of aromatic solvent (toluene) to act as a CO_2-soluble asphaltene stabilization agent capable of inhibiting asphaltene precipitation during immiscible CO_2 injection.[81]

Multiexponential analysis of the signal attenuation decays (eq 2) of the sealed samples delivers two values of diffusion coefficients, D_m and D_a, listed in Table 2 for different samples at fixed temperatures of 15 and 35 °C. Temperature dependencies of diffusion coefficients are presented in Figure 4. Since this is the first time the diffusion coefficients of asphaltene aggregates were measured in situ (under high-pressure CO_2), it is difficult to perform a direct comparison of the data obtained with those previously reported for asphaltene solutions under ambient conditions. However, some speculations can be made to provide an indirect assessment. Thus, translation dynamics depends on the geometry (size and shape) of the moving particle, the drag force of the surrounding media (i.e., its viscosity), and specific interactions between particle and environment. While the geometry and viscosity factors can be more or less scaled to high-pressure conditions, the specific interactions of aggregates with the environment in the presence of liquid CO_2 may not be similar to those in normal conditions. Nevertheless, scaling with measured diffusivity of water trace and solvent molecules gives diffusion coefficients of asphaltene aggregates in the range of $2-6 \times 10^{-10}$ m^2/s, which is very consistent with the values numerously reported for nanoaggregate diffusivity.[59−62] Also, it agrees well with the previously measured values for the same asphaltenes under ambient conditions.[63] Consequently, the diffusivity of the first component ("monomers") being an order of magnitude greater is consistent with those previously known.

Table 2. Diffusion Coefficients of the Asphaltene Monomers (D_m) and Aggregates (D_a) of the Asphaltene + Solvent + CO_2 Mixture Obtained at 15 and 35 °C

sample	D_m, 10^{-9} m^2/s 15°C	D_a, 10^{-10} m^2/s 15°C	D_m, 10^{-9} m^2/s 35°C	D_a, 10^{-10} m^2/s 35°C
Ch7	5.4	7.3	6.4	6.5
Ch25	5.3	8.8	6.7	10.1
Cd54	9.7	9.4	11.8	11.5
Ch150	6.1	8.1	7.2	10 (8.1)
B48	9.6	8.6	11.4	11.6

As is seen from the experimental data, a two-component nature of the diffusion curves along with a relatively high diffusivity value of aggregates (scaled to $2-6 \times 10^{-10}$ m^2/s) testify to the absence of macroaggregates (reported to have typical values of diffusion coefficients in the range of $0.3-0.6 \times 10^{-10}$ m^2/s).[63] This finding is intuitively expected due to the very low concentration of residual asphaltenes: the critical cluster concentration is reported to be around 10−20 g/L.[28] In addition to nanoaggregates, large asphaltene particles (flocs, with a characteristic size of up to a few micrometers) could be expectedly formed during flocculant-induced asphaltene precipitation. However, the mobility of asphaltene molecules in the large asphaltene particles probably becomes too slow, similar to that in the solid state. It is well-known that strong

https://doi.org/10.1021/acs.energyfuels.3c02862
Energy Fuels 2023, 37, 17215−17226

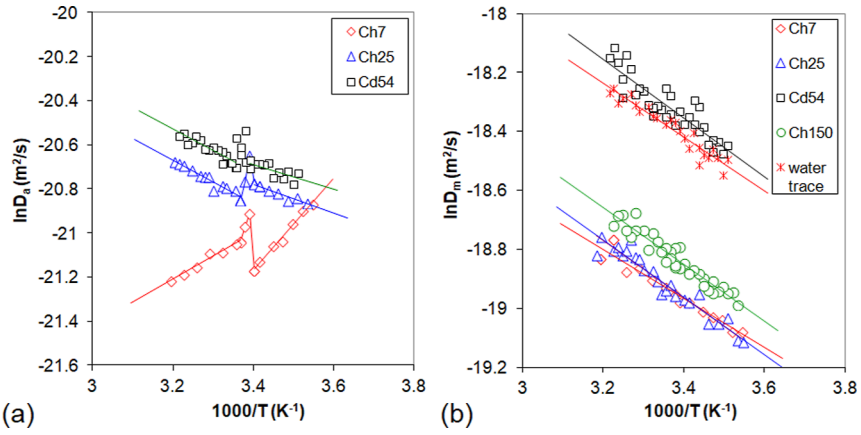

Figure 4. Temperature dependencies of diffusion coefficients of asphaltene aggregates (a) and monomers (b). The straight lines are the linear trends shown for visual guidance.

dipole−dipole interactions between immobilized protons and the presence of paramagnetic species reduce the apparent T_2 of asphaltenes from 30 to 80 ms in solution[80] to 0.2−1 ms in the solid state,[82] and even to tens of microseconds below glass transition temperature.[83,84] Consequently, the signal from the large asphaltene particles no longer contributes to diffusion attenuation curves, which are recorded with comparatively long gradient pulses, up to a few milliseconds (and delays up to hundreds of milliseconds). If one suppose retaining sufficient molecular mobility within the large flocs to provide long enough T_2, then according to the Stokes−Einstein equation, an increase in the size by three orders of magnitude (from 3 to 5 nm to 3−5 μm) caused a decrease of the diffusion coefficient in the same manner (i.e., slow down to 10^{-13} m^2/s), which would be clearly seen as a long fading tail in signal attenuation curves. Likely aggregated structures larger than nanoaggregates could have been formed during the preparation of the mixture. But after preparation, the flocs became precipitated due to the strong tendency of macroaggregates to further cluster until micron-sized particles under harsh conditions of high-pressure CO_2.

As mentioned above, the low viscosity of the media results in a sufficient (approximately by one order of magnitude) increase in diffusivity as compared to those found in normal asphaltene solutions. Yet the diffusivity usually increases with the increase in temperature due to a decrease in fluid viscosity. However, the results of diffusion measurements demonstrate an opposite trend of D_a for the sample Ch7 prepared from diluted asphaltene solution, Figure 4a, whereas diffusivities of either monomers or aggregates in any other samples follow a common trend.

The observed decrease of D_a for the Ch7 sample with temperature increase can occur in the following cases: the viscosity of the mixture increases, the hydrodynamic radius of asphaltene aggregates becomes larger, and intermolecular interactions between the surface of moving aggregates and the surrounding media become stronger. Because the other samples follow a common trend and the D_m of the Ch7 sample also increases with temperature, the viscosity factor can be eliminated, and the anomalous behavior of D_a should be attributed to the structure and dynamics of the aggregates. The increase of temperature evidently causes the growth of pressure inside the sealed capillary and the increase of the flocculating action of CO_2. It could lead to further destabilization of residual asphaltenes, followed by aggregate size increases and precipitation. The argument in favor of this suggestion is the decrease of weight fraction of aggregates, p_a, found for the Ch7 sample in the temperature range studied. The most likely growth of the aggregate size and decrease of fluid viscosity, being two independent factors affecting the apparent value of diffusivity, competitively result in a visible decline of D_a. In contrast to the Ch7 sample, aggregation processes in the Ch25 and Cd54 samples probably are not so intensive, and a factor of increasing the aggregate size is weaker than a factor of decreasing the fluid viscosity.

The effect of a temperature-dependent increase of aggregate size in the sample prepared from the most diluted asphaltene solution is not observed in other samples where it could be expected. It was previously established that the asphaltene concentration in solution determines the equilibrium of monomers-nanoaggregates and nanoaggregates-macroaggregates:[24,27,28,30,32−34] at low concentrations, below 10−20 g/L, the asphaltenes are mostly presented by nanoaggregates. At higher concentrations, the nanoaggregates begin to assemble into bigger units (macroaggregates), which stay in dynamic equilibrium with each other. Thus, when high-pressure CO_2 is introduced into the sample, the nanoaggregates turn out to be more stable than the macroaggregates, which likely precipitate first. Therefore, in the Ch7 sample, the aggregation process continues at a higher temperature/pressure, while in more concentrated samples, the majority of the asphaltenes, initially in the form of macroaggregates, have already become destabilized and precipitated. It can be concluded that CO_2-induced aggregation processes in diluted asphaltene solutions could unexpectedly appear even more pronounced than those in concentrated systems, depending on particular temperature and pressure conditions.

It is necessary to point out that the results obtained must be analyzed carefully to avoid some misleading conclusions. Thus, a comparison of the absolute values of D_a for different samples could indicate a clear direct proportionality between the diffusivity and the initial asphaltene concentration, Figure 4a. However, it is not the case: the D_a value is a complex product of several parameters, such as the viscosity of the system, which depends on both the initial asphaltene concentration and the mass fraction of CO_2 loaded; the size and weight fraction of aggregates, which also depend on the initial asphaltene concentration; and the dynamic equilibrium of monomer−aggregates and aggregates-deposit, which depends on temperature, pressure, solubility, etc. Moreover, the combination of all

https://doi.org/10.1021/acs.energyfuels.3c02862
Energy Fuels 2023, 37, 17215−17226

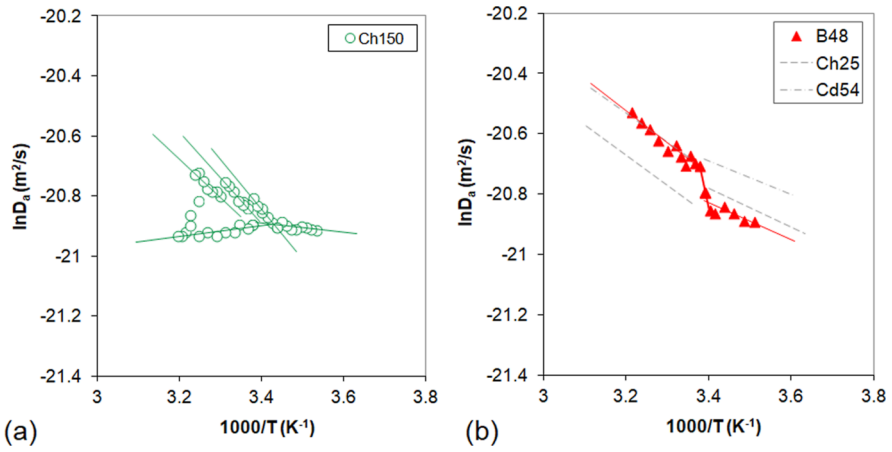

Figure 5. Temperature dependencies of diffusion coefficients of asphaltene aggregates in Ch150 (a) and B48 (b) samples. The straight solid lines are the linear trends shown for visual guidance; gray dotted lines are taken from the data of the Ch25 and Cd54 samples for better representativity.

these parameters has a positive feedback—changing the amount of CO_2 affects first the viscosity and then the amount of asphaltenes remaining in solution; the latter, in turn, changes the local viscosity and apparent D_a. A similar misunderstanding may appear when comparing the D_m, Figure 4b. It can be seen that the values of D_m for Ch7, Ch25, and Ch150 samples are close to each other, while for Cd54, they are much higher. It is partially due to the highest mass fraction of CO_2 loaded in this sample; also, there is no stabilizing additive (0.5 vol % of ethanol), which normally is presented in $CHCl_3$—the weight fraction of the monomers in Cd54 is small, and the first diffusion component becomes mostly presented by the water trace.

Another remarkable effect observed on temperature dependencies of diffusion coefficients of asphaltene aggregates is the abrupt change of D_a at a particular temperature, Figure 4a. For the Ch7 sample, this effect is most pronounced, occurring at 23 °C; for Ch25, the gap between the low and high temperature parts becomes smaller; and for the Cd54 sample, the gap is not even seen, but the change of slope retains. The temperature of the abrupt change slightly increases with the increase of the initial asphaltene concentration in the samples. Also, in the vicinity of this particular temperature point, the D_a beats (jumps above the trend) are clearly seen. Nothing similar was found on the temperature dependencies of D_m, ensuring that this effect comes from the asphaltene aggregates dynamics.

The abrupt change in slope of the temperature dependencies of diffusion coefficients, D_a, is very consistent with our previous findings obtained for the normal asphaltene solutions,[63] and it can be completely explained by temperature-triggered rearrangement of asphaltene aggregates. This structural transformation in asphaltene aggregates was first proposed by Evdokimov and coauthors; they performed the rheological experiments with unconventionally small temperature increments and observed noticeable structural transformations in asphaltene colloids, induced by comparatively small temperature variations within the range of 26−28 °C.[85,86] It was attributed to a first-order phase transition ascribed to an endothermic breakup of noncovalent (hydrogen) bonds in analogy with polymer particle shrinkage on heating that occurred at a specific "lower critical solution temperature" (LCST).[87−89] However, this brilliant finding was not confirmed until a comprehensive PFG NMR study of model asphaltene solutions proved that the temperature-triggered reorganization of hydrogen bonding, being a general physical process not ultimately limited to LCST cases, is also an intrinsic property of asphaltene aggregate structure (a very detailed description of the concept of endothermic breakup of noncovalent bonds and its effect on aggregate dynamics can be found in ref 63). The results of the current work evidence that under high-pressure CO_2 conditions, the structural transformations of asphaltene aggregates are not hindered, but instead, they become even more highlighted due to the higher sensitivity of translational dynamics to the smallest changes of the aggregate architecture in the low-viscosity surroundings. It can be concluded that the recent "supramolecular assembly" concept,[90] which strengthens the role of hydrogen (and other noncovalent) bonding in overall aggregation processes, can be extended to high-pressure CO_2 conditions.

Similarly to the Ch7 sample prepared from the most diluted asphaltene solution, the Ch150 sample prepared from the most concentrated solution shows a very peculiar behavior of diffusion coefficients, Figure 5a. As can be seen, there is not only the change in slope of temperature dependence of diffusion coefficients at ∼20 °C but also a series of less pronounced transformations at 23 and 29 °C, appearing in the form of small jumps in D_a values. When the temperature of the sample reaches 35−37 °C, the diffusion coefficients suddenly drop and begin following another temperature trend upon cooling the sample. Moving down, this trend comes into the first transformation point at 20 °C, demonstrating a hysteresis behavior never observed in any other samples.

It is difficult to provide a clear and consistent explanation for the unusual diffusion behavior of asphaltene aggregates in the Ch150 sample. The only evident thing is that the complexity of behavior probably stems from the initial conditions presented in very a concentrated asphaltene solution. At very high concentrations, >10 wt %, the majority of asphaltene molecules are certainly assembled into macroaggregates, which are then destabilized and precipitated under the action of CO_2 introduced during sample preparation. Also, the mass fraction of CO_2 injected appears relatively low (Table 1), making the flocculating strength of the media weaker. A combination of these two factors may result in a relatively slow increase in aggregates size upon an increase of temperature (and pressure), which is accompanied by some steplike changes of particles size at specific temperatures, visible as small jumps of D_a. From this point of view, the hysteresis can be a result of the

https://doi.org/10.1021/acs.energyfuels.3c02862
Energy Fuels 2023, 37, 17215−17226

better stability of the aggregates: comparatively larger particles no longer precipitate at ~40 °C, and when the temperature decreases, they are kept assembled for some temperature range.

As described above, PFG NMR measurements in the B48 sample revealed a smaller weight fraction of the aggregate component as compared to those in Ch/Cd samples. Moreover, the temperature dependence of diffusion coefficients also differs, though they demonstrate similar trends. Thus, the absolute values of D_a are close to those in previously discussed samples, and they also increase as temperature increases with a similar slope of the linear trends, Figure 5b. However, the structural transformation at 21−23 °C appears much more pronounced than those in Ch25 and Cd54 samples, jumping over their difference: the distance between the low- and high-temperature branches of the dependence (B48 sample) is equal to the difference between values of D_a for those two (Ch25 and Cd54) samples. In comparison, the diffusion appearance of temperature-triggered rearrangement of asphaltene aggregates in the B48 sample is more similar to those in the Ch7 sample, which probably is the result of a larger fraction of nanoaggregates in initial asphaltene solutions—in Ch7, it is due to dilution, while in B48, it is due to the nature of the aromatic solvent. Very similar conditions, such as the initial asphaltene concentration in solution and the amount of CO_2 loaded, result in rather different asphaltene aggregate dynamics of the samples Cd54 and B48 due to the different natures of the solvents used. Along with the conclusion on CO_2-induced aggregation processes in diluted asphaltene solutions that turned out to be somewhat more pronounced than those in concentrated systems, it can be stated that the scenario according to which the evolution of the asphaltene aggregates will develop strongly depends on the initial concentration of dissolved asphaltenes, the mass fraction of CO_2 loaded into the system, and the nature of the media where the aggregation occurs.

4. CONCLUSIONS

In the present work, the first in situ PFG NMR study of asphaltene aggregates behavior under high-pressure CO_2 was carried out. For this purpose, a series of sealed, thick-walled quartz capillaries were prepared where carbon dioxide was loaded into asphaltene solution under high pressure. By means of PFG NMR, the translational dynamics of diffusing species was measured in the 8−42 °C temperature range for samples with different initial asphaltene concentrations and types of solvent. The introduction of high-pressure CO_2 into the asphaltene solution caused asphaltene destabilization and precipitation. According to ^{1}H spectroscopic data, it was found that the residual asphaltene concentration in the sealed capillaries did not exceed 2−4 g/L, ensuring sufficient deposition of the asphaltenes and a high degree of dilution of the studied samples. Also, proton NMR spectra revealed an increase in the share of asphaltene molecules, which remained dissolved with a more branched "archipelago" structure.

Despite a quite low asphaltene concentration, experimental data clearly demonstrated the presence of aggregated structures attributed solely to nanoaggregates, with no signs of the presence of macroaggregates in the samples. Multiexponential analysis of the experimental signal attenuation curves revealed a very high weight fraction of the aggregate component, up to 70−80%, in chloroform solution, while those in benzene solution appear much lower, 40−50%, indicating better affinity of the aromatic solvent to asphaltenes even in high-pressure CO_2 environments, which can be potentially used in a field practice for inhibiting asphaltene precipitation during CO_2-EOR.

Temperature dependencies of aggregate diffusivity clearly showed the strong influence of the initial asphaltene concentration, mass fraction of CO_2 loaded into the system, and chemical nature of the solvent used on the evolution of the aggregates and their local dynamics. In particular, the most diluted asphaltene solution, expected to be the most resistive to aggregation processes under high-pressure CO_2 conditions, revealed the most pronounced aggregation-dependent translational dynamics as compared to those with a moderate initial asphaltene concentration. Yet, even the extremely concentrated asphaltene solution may not show drastic aggregation processes if the mass fraction of the CO_2 loaded does not appear so high. By comparing the effects of chloroform and benzene, it was also established that very similar conditions, such as initial asphaltene concentration and amount of CO_2 loaded, nevertheless may result in rather different asphaltene aggregate dynamics due to the different natures of the solvents used.

Finally, the experimental data evidence that in a high-pressure CO_2 environment, the temperature-triggered structural transformation of asphaltene aggregates due to the noncovalent bond breakup is not hindered but instead becomes more emphasized due to the higher sensitivity of the translational dynamics of aggregates to the smallest changes in their architecture. It means that harsh high-pressure CO_2 conditions have virtually no extinguishing effect on intermolecular hydrogen bonding, and the concept of supramolecular assembly of asphaltene aggregates can be extended to aggregation processes, which may happen during CO_2-EOR. The results obtained shed new light on asphaltene aggregate dynamics and brought new knowledge about the fundamental behavior of asphaltene in high-pressure CO_2 conditions. They contribute to the overall understanding of the complex and versatile phenomenon of asphaltene precipitation and hopefully will assist in better prediction of reservoir performance during CO_2-EOR.

AUTHOR INFORMATION

Corresponding Author

Evgeny V. Morozov − *Institute of Chemistry and Chemical Technology, Federal Research Center "Krasnoyarsk Science Center of Siberian Branch of the Russian Academy of Sciences", Krasnoyarsk 660036, Russia; Kirensky Institute of Physics, Federal Research Center "Krasnoyarsk Science Center of Siberian Branch of the Russian Academy of Sciences", Krasnoyarsk 660036, Russia; Federal Research Center "Krasnoyarsk Science Center of Siberian Branch of the Russian Academy of Sciences", Krasnoyarsk 660036, Russia;* orcid.org/0000-0003-1561-3937; Email: morozovev@iph.krasn.ru

Authors

Sergey N. Trukhan − *Boreskov Institute of Catalysis, Siberian Branch of the Russian Academy of Sciences, Novosibirsk 630090, Russia; Federal Research Center "Krasnoyarsk Science Center of Siberian Branch of the Russian Academy of Sciences", Krasnoyarsk 660036, Russia;* orcid.org/0000-0001-8403-5902

https://doi.org/10.1021/acs.energyfuels.3c02862
Energy Fuels 2023, 37, 17215−17226

Ivan V. Kozhevnikov − *Boreskov Institute of Catalysis, Siberian Branch of the Russian Academy of Sciences, Novosibirsk 630090, Russia; Federal Research Center "Krasnoyarsk Science Center of Siberian Branch of the Russian Academy of Sciences", Krasnoyarsk 660036, Russia;* orcid.org/0000-0002-0252-5850

Ivan V. Peterson − *Institute of Chemistry and Chemical Technology, Federal Research Center "Krasnoyarsk Science Center of Siberian Branch of the Russian Academy of Sciences", Krasnoyarsk 660036, Russia; Federal Research Center "Krasnoyarsk Science Center of Siberian Branch of the Russian Academy of Sciences", Krasnoyarsk 660036, Russia*

Oleg N. Martyanov − *Boreskov Institute of Catalysis, Siberian Branch of the Russian Academy of Sciences, Novosibirsk 630090, Russia;* orcid.org/0000-0001-9999-8680

Complete contact information is available at: https://pubs.acs.org/10.1021/acs.energyfuels.3c02862

Notes

The authors declare no competing financial interest.

■ ACKNOWLEDGMENTS

The present research was performed with the financial support of the Russian Science Foundation (project no. 21-13-00171, http://rscf.ru/project/21-13-00171/) using the equipment of the Krasnoyarsk Regional Center of Research Equipment of the Federal Research Center "Krasnoyarsk Science Center SB RAS".

■ REFERENCES

(1) Bahadori, A. *Fundamentals of Enhanced Oil and Gas Recovery from Conventional and Unconventional Reservoirs*; Elsevier, Gulf Professional Publishing: UK, 2018; p 536..

(2) Alagorni, A. H.; Yaacob, Z. B.; Nour, A. H. An Overview of Oil Production Stages: Enhanced Oil Recovery Techniques and Nitrogen Injection. *Int. J. Environ. Sci. Dev.* **2015**, *6* (9), 693−701.

(3) Nabipour, M.; Escrochi, M.; Ayatollahi, S.; Boukadi, F.; Wadhahi, M.; Maamari, R.; Bemani, A. Laboratory investigation of thermally-assisted gas-oil gravity drainage for secondary and tertiary oil recovery in fractured models. *J. Pet. Sci. Eng.* **2007**, *55*, 74−82.

(4) Nobakht, M.; Moghadam, S.; Gu, Y. Mutual interactions between crude oil and CO2 under different pressures. *Fluid Phase Equilib.* **2008**, *265*, 94−103.

(5) van Poollen, H. K. *Fundamentals of Enhanced Oil Recovery*; Pennwell Books: Tulsa, United States, 1980; p 155.

(6) Alvarado, V.; Manrique, E. Enhanced Oil Recovery: An Update Review. *Energies* **2010**, *3*, 1529−1575.

(7) Green, D. W.; Willhite, G. P. *Enhanced Oil Recovery, 2nd* ed.; Society of Petroleum Engineers: Richardson, TX, 2018; p 896..

(8) https://www.energy.gov/fecm/enhanced-oil-recovery (accessed Oct 08, 2023).

(9) Holm, L. W.; Josendal, V. A. Mechanisms of oil displacement by carbon dioxide. *J. Pet. Technol.* **1974**, *26* (12), 1427−1438.

(10) Blunt, M.; Fayers, F. J.; Orr, F. M. Carbon dioxide in enhanced oil recovery. *Energy Convers. Manage.* **1993**, *34*, 1197−1204.

(11) Meng, X.; Sheng, J. J.; Yu, Y. Experimental and numerical study of enhanced condensate recovery by gas injection in shale gas-condensate reservoirs. *Soc. Pet. Eng.* **2017**, *20* (02), 471−477.

(12) Tan, Y.; Li, Q.; Xu, L.; Ghaffar, A.; Zhou, X.; Li, P. A critical review of carbon dioxide enhanced oil recovery in carbonate reservoirs. *Fuel* **2022**, *328*, 125256.

(13) Mungan, N. Carbon dioxide flooding - fundamentals. *J. Can. Pet. Technol.* **1984**, *20* (1), 131−176.

(14) Farajzadeh, R.; Andrianov, A.; Bruining, H.; Zitha, P. L. J. Comparative Study of CO2 and N2 Foams in Porous Media at Low and High Pressure-Temperatures. *Ind. Eng. Chem. Res.* **2009**, *48*, 4542−4552.

(15) Aycaguer, A. C.; Lev-On, M.; Winer, A. M. Reducing carbon dioxide emissions with enhanced oil recovery projects: a life cycle assessment approach. *Energy Fuels* **2001**, *15* (2), 303−308.

(16) Godec, M. L.; Kuuskraa, V. A.; Dipietro, P. Opportunities for Using Anthropogenic CO2 for Enhanced Oil Recovery and CO2 Storage. *Energy Fuels* **2013**, *27* (8), 4183−4189.

(17) Kokal, S. L.; Sayegh, S. G. Asphaltenes: the cholesterol of petroleum. *Presented at SPE Middle East Oil Show*: Manama, Bahrain, 1995..

(18) Leontaritis, K. J.; Ali Mansoori, G. Asphaltene deposition: a survey of field experiences and research approaches. *J. Pet. Sci. Eng.* **1988**, *1*, 229−239.

(19) Eskin, D.; Mohammadzadeh, O.; Akbarzadeh, K.; Taylor, S. D.; Ratulowski, J. Reservoir Impairment by Asphaltenes: A Critical Review. *Can. J. Chem. Eng.* **2016**, *94*, 1202−1217.

(20) Almehaideb, R. A. Asphaltene precipitation and deposition in the near wellbore region: a modeling approach. *J. Pet. Sci. Eng.* **2004**, *42*, 157−170.

(21) Ju, B.; Fan, T.; Jiang, Z. Modeling asphaltene precipitation and flow behavior in the processes of CO2 flood for enhanced oil recovery. *J. Pet. Sci. Eng.* **2013**, *109*, 144−154.

(22) Jafari Behbahani, T.; Ghotbi, C.; Taghikhani, V.; Shahrabadi, A. Investigation of asphaltene adsorption in sandstone core sample during CO2 injection: experimental and modified modeling. *Fuel* **2014**, *133*, 63−72.

(23) Song, Z.; Zhu, W.; Wang, X.; Guo, S. 2-D pore-scale experimental investigations of asphaltene deposition and heavy oil recovery by CO2 flooding. *Energy Fuels* **2018**, *32*, 3194−3201.

(24) Mullins, O. C.; Sheu, E. Y.; Hammami, A.; Marshall, A. G. *Asphaltenes, Heavy Oils, and Petroleomics*; Springer: New York, 2007; p 670.

(25) Speight, J. G. *The Chemistry and Technology of Petroleum*, 4th ed.; Taylor & Francis: Hoboken, 2006; p 984.

(26) Groenzin, H.; Mullins, O. C. Molecular size and structure of asphaltenes from various sources. *Energy Fuels* **2000**, *14*, 677−684.

(27) Mullins, O. C.; Sabbah, H.; Eyssautier, J.; Pomerantz, A. E.; Barré, L.; Andrews, A. B.; Ruiz-Morales, Y.; Mostowfi, F.; McFarlane, R.; Goual, L.; et al. Advances in asphaltene science and the Yen-Mullins model. *Energy Fuels* **2012**, *26*, 3986−4003.

(28) Mullins, O. C. The asphaltenes. *Annu. Rev. Anal. Chem.* **2011**, *4*, 393−418.

(29) Fenistein, D.; Barre, L. Experimental measurement of the mass distribution of petroleum asphaltene aggregates using ultracentrifugation and small-angle X-ray scattering. *Fuel* **2001**, *80*, 283−287.

(30) Zeng, H.; Song, Y. Q.; Johnson, D. L.; Mullins, O. C. Critical Nanoaggregate Concentration of Asphaltenes by Direct-Current (DC) Electrical Conductivity. *Energy Fuels* **2009**, *23*, 1201−1208.

(31) Evdokimov, I. N.; Fesan, A. A. Multi-step formation of asphaltene colloids in dilute solutions. *Colloids Surf., A* **2016**, *492*, 170−180.

(32) Goual, L.; Sedghi, M.; Zeng, H.; Mostowfi, F.; McFarlane, R.; Mullins, O. C. On the Formation and Properties of Asphaltene Nanoaggregates and Clusters by DC-Conductivity and Centrifugation. *Fuel* **2011**, *90*, 2480−2490.

(33) Hoepfner, M. P.; Fogler, H. S. Multiscale Scattering Investigations of Asphaltene Cluster Breakup, Nanoaggregate Dissociation, and Molecular Ordering. *Langmuir* **2013**, *29*, 15423−15432.

(34) Hoepfner, M. P.; Vilas Bôas Fávero, C.; Haji-Akbari, N.; Fogler, H. S. The Fractal Aggregation of Asphaltenes. *Langmuir* **2013**, *29*, 8799−8808.

(35) Espinat, D.; Fenistein, D.; Barre, L.; Frot, D.; Briolant, Y. Effects of Temperature and Pressure on Asphaltenes Agglomeration in Toluene. A Light, X-ray, and Neutron Scattering Investigation. *Energy Fuels* **2004**, *18*, 1243−1249.

(36) Mansur, C. R.; de Melo, A. R.; Lucas, E. F. Determination of asphaltene particle size: influence of flocculant, additive, and temperature. *Energy Fuels* **2012**, *26*, 4988−4994.
(37) Morozov, E. V.; Martyanov, O. N. Probing Flocculant-Induced Asphaltene Precipitation Via NMR Imaging: From Model Toluene-Asphaltene Systems To Natural Crude Oils. *Appl. Magn. Reson.* **2016**, *47*, 223−235.
(38) Nguele, R.; Ghulami, M. R.; Sasaki, K.; Said-Al Salim, H.; Widiatmojo, A.; Sugai, Y.; Nakano, M. Asphaltene Aggregation in Crude Oils during Supercritical Gas Injection. *Energy Fuels* **2016**, *30*, 1266−1278.
(39) Zanganeh, P.; Dashti, H.; Ayatollahi, S. Visual investigation and modeling of asphaltene precipitation and deposition during CO2 miscible injection into oil reservoirs. *Fuel* **2015**, *160*, 132−139.
(40) Dashti, H.; Zanganeh, P.; Kord, S.; Ayatollahi, S.; Amiri, A. Mechanistic study to investigate the effects of different gas injection scenarios on the rate of asphaltene deposition: An experimental approach. *Fuel* **2020**, *262*, 116615.
(41) Srivastava, R. K.; Huang, S. S. Asphaltene Deposition During CO2 Flooding: A Laboratory Assessment. *Paper Presented at the SPE Production Operations Symposium*: Oklahoma City, Oklahoma, 1997..
(42) Soroush, S.; Pourafshary, P.; Vafaie-Sefti, M. A Comparison of Asphaltene Deposition in Miscible and Immiscible Carbon Dioxide Flooding in Porous Media. *Paper Presented at the SPE EOR Conference at Oil and Gas West Asia*: Muscat, Oman, 2014..
(43) Deo, M.; Parra, M. Characterization of Carbon-Dioxide-Induced Asphaltene Precipitation. *Energy Fuels* **2012**, *26*, 2672−2679.
(44) Cruz, A. A.; Amaral, M.; Santos, D.; Palma, A.; Franceschi, E.; Borges, G. R.; Coutinho, J. A. P.; Palácio, J.; Dariva, C. CO_2 influence on asphaltene precipitation. *J. Supercrit. Fluids* **2019**, *143*, 24−31.
(45) da Silva, N. A. E.; Oliveira, V. d. R.; Souza, M. M. S.; Guerrieri, Y.; Costa, G. M. N. New method to detect asphaltene precipitation onset induced by CO2 injection. *Fluid Phase Equilib.* **2014**, *362*, 355−364.
(46) Idem, R. O.; Ibrahim, H. H. Kinetics of CO2-induced asphaltene precipitation from various Saskatchewan crude oils during CO2 miscible flooding. *J. Pet. Sci. Eng.* **2002**, *35*, 233−246.
(47) Zanganeh, P.; Ayatollahi, S.; Alamdari, A.; Zolghadr, A.; Dashti, H.; Kord, S. Asphaltene Deposition during CO2 Injection and Pressure Depletion: A Visual Study. *Energy Fuels* **2012**, *26*, 1412−1419.
(48) Verdier, S.; Carrier, H.; Andersen, S. I.; Daridon, J.-L. Study of Pressure and Temperature Effects on Asphaltene Stability in Presence of CO_2. *Energy Fuels* **2006**, *20*, 1584−1590.
(49) Ibrahim, H. H.; Idem, R. O. Correlations of Characteristics of Saskatchewan Crude Oils/Asphaltenes with Their Asphaltenes Precipitation Behavior and Inhibition Mechanisms: Differences between CO_2- and n-Heptane-Induced Asphaltene Precipitation. *Energy Fuels* **2004**, *18*, 1354−1369.
(50) Soorghali, F.; Zolghadr, A.; Ayatollahi, S. Effect of Resins on Asphaltene Deposition and the Changes of Surface Properties at Different Pressures: A Microstructure Study. *Energy Fuels* **2014**, *28*, 2415−2421.
(51) Sedghi, M.; Goual, L. Role of resins on asphaltene stability. *Energy Fuels* **2010**, *24* (4), 2275−2280.
(52) Pereira, J. C.; López, I.; Salas, R.; Silva, F.; Fernández, C.; Urbina, C.; López, J. C. Resins: The molecules responsible for the stability/instability phenomena of asphaltenes. *Energy Fuels* **2007**, *21* (3), 1317−1321.
(53) Liu, B.; Li, J.; Qi, C.; Li, X.; Mai, T.; Zhang, J. Mechanism of asphaltene aggregation induced by supercritical CO2: insights from molecular dynamics simulation. *RSC Adv.* **2017**, *7*, 50786−50793.
(54) Gabrienko, A. A.; Martyanov, O. N.; Kazarian, S. G. Behavior of Asphaltenes in Crude Oil at High-Pressure CO2 Conditions: In Situ Attenuated Total Reflection-Fourier Transform Infrared Spectroscopic Imaging Study. *Energy Fuels* **2016**, *30*, 4750−4757.
(55) Joonaki, E.; Buckman, J.; Burgass, R.; Tohidi, B. Exploration of the difference in molecular structure of n -C7 and CO_2 induced asphaltenes. *Ind. Eng. Chem. Res.* **2018**, *57*, 8810−8818.
(56) Afra, S.; Samouei, H.; Golshahi, N.; Nasr-El-Din, H. Alterations of asphaltenes chemical structure due to carbon dioxide injection. *Fuel* **2020**, *272*, 117708.
(57) Martyanov, O. N.; Larichev, Y. V.; Morozov, E. V.; Trukhan, S. N.; Kazarian, S. G. The stability and evolution of oil systems studied via advanced methods in situ. *Russ. Chem. Rev.* **2017**, *86*, 999−1023.
(58) Price, W. S. *NMR Studies of Translational Motion: Principles and Applications*; Cambridge University Press: Cambridge, UK, 2009; p 393.
(59) Kawashima, H.; Takanohashi, T.; Iino, M.; Matsukawa, S. Determining Asphaltene Aggregation in Solution from Diffusion Coefficients As Determined by Pulsed-Field Gradient Spin-Echo 1H NMR. *Energy Fuels* **2008**, *22*, 3989−3993.
(60) Durand, E.; Clemancey, M.; Lancelin, J.-M.; Verstraete, J.; Espinat, D.; Quoineaud, A.-A. Aggregation states of asphaltenes: Evidence of two chemical behaviors by 1H diffusion-ordered spectroscopy nuclear magnetic resonance. *J. Phys. Chem. C* **2009**, *113*, 16266−16276.
(61) Lisitza, N. V.; Freed, D. E.; Sen, P. N.; Song, Y.-Q. Study of Asphaltene Nanoaggregation by Nuclear Magnetic Resonance (NMR). *Energy Fuels* **2009**, *23*, 1189−1193.
(62) Durand, E.; Clemancey, M.; Lancelin, J.-M.; Verstraete, J.; Espinat, D.; Quoineaud, A.-A. Effect of Chemical Composition on Asphaltenes Aggregation. *Energy Fuels* **2010**, *24*, 1051−1062.
(63) Morozov, E. V.; Yushmanov, P. V.; Martyanov, O. N. Temperature-Triggered Rearrangement of Asphaltene Aggregates as Revealed by Pulsed-Field Gradient NMR. *Energy Fuels* **2019**, *33*, 6934−6945.
(64) Yoshida, K.; Wakai, C.; Matubayasi, N.; Nakahara, M. A New High-Temperature Multinuclear-Magnetic-Resonance Probe and the Self-Diffusion of Light and Heavy Water in Sub- and Supercritical Conditions. *J. Chem. Phys.* **2005**, *123* (16), 164506.
(65) Xu, B.; Nagashima, K.; DeSimone, J. M.; Johnson, C. S. Diffusion of Water in Liquid and Supercritical Carbon Dioxide: An NMR Study. *J. Phys. Chem. A* **2003**, *107* (1), 1−3.
(66) *ASTM D6560, Standard Test Method for Determination of Asphaltenes (Heptane Insolubles) in Crude Petroleum and Petroleum Products*; ASTM International: West Conshohocken, PA, 2012. http://www.astm.org/Standards/D6560.htm.
(67) Kozhevnikov, I. V.; Nuzhdin, A. L.; Martyanov, O. N. Transformation of petroleum asphaltenes in supercritical water. *J. Supercrit. Fluids* **2010**, *55* (1), 217−222.
(68) Trukhan, S. N.; Kazarian, S. G.; Martyanov, O. N. Electron spin resonance of slowly rotating vanadyls-effective tool to quantify the sizes of asphaltenes in situ. *Energy Fuels* **2017**, *31* (1), 387−394.
(69) Larichev, Y. V.; Nartova, A. V.; Martyanov, O. N. The influence of different organic solvents on the size and shape of asphaltene aggregates studied via small-angle X-ray scattering and scanning tunneling microscopy. *Adsorpt. Sci. Technol.* **2016**, *34* (2−3), 244−257.
(70) Trukhan, S. N.; Yakushkin, S. S.; Martyanov, O. N. Fine-Tuning Simulation of the ESR Spectrum-Sensitive Tool to Identify the Local Environment of Asphaltenes in Situ. *J. Phys. Chem. C* **2022**, *126* (26), 10729−10741.
(71) Morozov, E. V.; Nizovtseva, P. V.; Martyanov, O. N. From Components to Phase-Dependent Dynamics of Diffusivity in Wax Solutions Subjected to Fluid-Solid Phase Transition: Insights from Pulsed Field Gradient NMR. *Energy Fuels* **2022**, *36* (24), 14696−14709.
(72) Stejskal, E. O.; Tanner, J. E. Spin diffusion measurements: spin echoes in the presence of a time - dependent field gradient. *J. Chem. Phys.* **1965**, *42*, 288−292.
(73) Ostlund, J.-A.; Nyden, M.; Stilbs, P. Component-Resolved Diffusion in Multicomponent Mixtures. A Case Study of High-Field PGSE-NMR Self-Diffusion Measurements in Asphaltene/Naphthenic Acid/Solvent Systems. *Energy Fuels* **2004**, *18*, 531−538.
(74) Ok, S.; Mal, T. K. NMR Spectroscopy Analysis of Asphaltenes. *Energy Fuels* **2019**, *33* (11), 10391−10414.

(75) Santos Silva, H.; Sodero, A. C. R.; Korb, J.-P.; Alfarra, A.; Giusti, P.; Vallverdu, G.; Bégué, D.; Baraille, I.; Bouyssiere, B. The role of metalloporphyrins on the physical-chemical properties of petroleum fluids. *Fuel* **2017**, *188*, 374−381.
(76) Trukhan, S. N.; Morozov, E. V.; Martyanov, O. N. Resin-Paraffin Aggregation Processes in Waxy Oil Revealed by Vanadyl Porphyrin Spin Probe. *Energy Fuels* **2023**, *37* (16), 11797−11806.
(77) Liu, H.; Wang, Z.; Guo, A.; Lin, C.; Chen, K. The Distribution of Ni and V in Resin and Asphaltene Subfractions and Its Variation During Thermal Processes. *Pet. Sci. Technol.* **2015**, *33* (2), 203−210.
(78) Yakubov, M. R.; Sinyashin, K. O.; Abilova, G. R.; Tazeeva, E. G.; Milordov, D. V.; Yakubova, S. G.; Borisov, D. N.; Gryaznov, P. I.; Mironov, N. A.; Borisova, Y. Differentiation of heavy oils according to the vanadium and nickel content in asphaltenes and resins. *Petrochem* **2017**, *57*, 849−854.
(79) Rodionov, A.; Mukhamatdinov, I.; Mamin, G.; Gafurov, M.; Orlinskii, S.; Salih, I.; Vakhin, A. Distribution of vanadyl complexes and free radicals in asphaltenes fractions from electron paramagnetic resonance. *IOP Conf. Ser.: Earth Environ. Sci.* **2019**, *282*, 012008.
(80) Dutta Majumdar, R.; Gerken, M.; Mikula, R.; Hazendonk, P. Validation of the Yen-Mullins Model of Athabasca Oil-Sands Asphaltenes using Solution-State 1H NMR Relaxation and 2D HSQC Spectroscopy. *Energy Fuels* **2013**, *27* (11), 6528−6537.
(81) Gandomkar, A.; Torabi, F.; Nasriani, H. R.; Enick, R. M. Decreasing Asphaltene Precipitation and Deposition during Immiscible Gas Injection Via the Introduction of a CO2-Soluble Asphaltene Inhibitor. *SPE J.* **2023**, *28* (05), 2316−2328.
(82) Dutta Majumdar, R.; Montina, T.; Mullins, O. C.; Gerken, M.; Hazendonk, P. Insights into asphaltene aggregate structure using ultrafast MAS solid-state 1H NMR spectroscopy. *Fuel* **2017**, *193*, 359−368.
(83) Shkalikov, N. V.; Ganeeva, Y. M.; Yusupova, T. N.; Skirda, V. D. The characterization of asphaltenes by 1H NMR relaxation method: microsecond range of spin-spin relaxation times. *Magn. Reson. Solids* **2008**, *10* (1), 11−19.
(84) Ivanov, D. S.; Barskaya, E. E.; Skirda, V. D. Size effect for asphaltene particles in the resin by NMR. *Magn. Reson. Solids* **2019**, *21*, 19201.
(85) Evdokimov, I. N.; Eliseev, N. Y.; Eliseev, D. Y. Rheological evidence of structural phase transitions in asphaltene-containing petroleum fluids. *J. Pet. Sci. Eng.* **2001**, *30*, 199−211.
(86) Evdokimov, I. N.; Eliseev, N. Y. Thermally Responsive Properties of Asphaltene Dispersions. *Energy Fuels* **2006**, *20*, 682−687.
(87) Zhang, J. *Switchable and Responsive Surfaces and Materials for Biomedical Applications*; Elsevier, Woodhead Publishing: Cambridge, UK, 2015; p 324.
(88) Ahn, S.; Kasi, R. M.; Kim, S.-C.; Sharma, N.; Zhou, Y. Stimuli responsive polymer gels. *Soft Matter* **2008**, *4*, 1151−1157.
(89) Yushmanov, P. V.; Furo, I.; Iliopoulos, I. Kinetics of Demixing and Remixing Transitions in Aqueous Solutions of Poly-(Nisopropylacrylamide): A Temperature-Jump 1H NMR Study. *Macromol. Chem. Phys.* **2006**, *207*, 1972−1979.
(90) Gray, M. R.; Tykwinski, R. R.; Stryker, J. M.; Tan, X. Supramolecular Assembly Model for Aggregation of Petroleum Asphaltenes. *Energy Fuels* **2011**, *25*, 3125−3134.

https://doi.org/10.1021/acs.energyfuels.3c02862
Energy Fuels 2023, 37, 17215−17226